Theoretical investigation of ignition with lasers

Donghua Fang (方栋华), Yang Xie (谢 阳), Zhiyan Ma (马志炎),
Jianqin Wei (魏建勤), and Cangsu Xu (许沧粟)*

Institute of Power-driven Machinery and Vehicle Engineering, Zhejiang University, Hangzhou 310027, China

**Corresponding author: xcs0929@163.com*

Received April 10, 2012; accepted July 23, 2012; posted online December 5, 2012

A fundamental theoretical investigation of laser ignition is reported. Ignition is happened in an explosion bomb which equipped with visualization windows and all aspects of the phenomenon such as plasmas, shock waves, ignition kernels, and propagating flames are observed by high-speed schlieren photography. The study covers different phases of laser ignition with theoretical interpretations in chronological order, consisting of electrical breakdown and energy transfer from laser to plasma, shock-wave generation and propagation, gasdynamic effects and generation of the third lobe, chemical induction and ignition and turbulent flame initiation.

OCIS codes: 140.0140, 020.0020.
doi: 10.3788/COL201210Sl.S21414.

Laser ignition has become an active research topic in recent years. Compared with conventional spark ignition, laser ignition displays a number of advantages. It is accomplished without electrodes. The rate of energy, which transfered from the beam, can be extremely high and localized, laser wavelengths can be tuned to particular molecular energy levels, and the location for breakdown can be selected. Furthermore, the subsequent speed of flame propagation can be enhanced after laser ignition.

Laser ignition of reactive mixtures can be divided into four categories[1] as follows.

a) Laser thermal ignition

Thermal ignition uses a laser beam to increase the kinetic energy of the target molecules in either translational, rotational, or vibrational form. As a result, the molecular bonds are broken and chemical reactions occur. The ignition delay time is typically long.

b) Laser-induced photochemical ignition

In this ignition mechanism, laser photons dissociate the target molecules into highly reactive radical species. If the production rates of these radicals are greater than their recombination rates, they will initiate the usual chemical chain-branching reactions leading to ignition and full-scale combustion.

c) Laser-induced resonant breakdown

From the physical standpoint, this process involves the non-resonant multiphoton photodissociation of some of the molecules in the gas mixture, and the resonant photoionization of one or more atoms generated by the photodissociation process. The sequence of these two processes leads to the formation of seed electrons, which can then readily absorb more energy by the inverse bremsstrahlung effect leading to the formation of plasmas leading to ignition.

d) The laser-induced spark ignition

Laser-induced ignition depends upon electrical breakdown. Initially, multi-photon ionization of few gas molecules which releases electrons that readily absorb more photons via the inverse bremsstrahlung process to increase their kinetic energy. Electrons liberated by this means collide with other molecules and ionize them, leading to an electron avalanche, and breakdown the gas. Then with high temperature and pressure the highly reactive chemical intermediates produce spark. If the spark is intense enough, then the resultant ignition kernel is sufficiently strong to permit transition into full scale combustion.

In this letter, we state the laser-induced spark ignition and discuss the different phases of laser ignition in chronological order including electrical breakdown and energy transfer from laser to plasma, shock-wave generation and propagation, gasdynamic effects and generation of the third lobe, chemical induction and ignition and turbulent flame initiation found by Bradley *et al.*[2].

It is certain that laser-induced ignition depends upon electrical breakdown which is similar to that of an electric spark discharge. However, laser-induced sparks are smaller, larger temperature, and density gradients, and more transient in nature[1]. Initially, in laser-induced ignition a gas molecule or atom simultaneously absorbs a number of photons. The gas molecule is ionized when the absorbed energy is higher than its ionization potentia. Multiphoton ionization generates electrons that are accelerated to energies high enough to create further ionization. The next process of electron requires the existence of initial electrons when the laser irradiance is high enough. The generation of the initial electrons is also influenced by the presence of impurities, such as aerosol particles or low ionization-potential organic vapors. The electrons then absorb more photons via the inverse bremsstrahlung process. If the electrons gain sufficient energy, they ionize other gas molecules on impact, leading to an electron cascade and breakdown of the gas.

The probability and threshold energy of breakdown have been studied by many authors. The electrical breakdown is enhanced at high pressure by the increased collision frequencies. This explains the associated decrease in breakdown energy in Fig. 1[2]. They think the greater sensitivity of the probability of breakdown to pressure at low pressure might be due to shot-to-shot variation in the output laser beam, associated with changes in the modal structure of the laser. They also found variation of breakdown threshold energy with pressure in different mixtures shown in Fig. 2. No significant differences were observed in the breakdown threshold between lean and

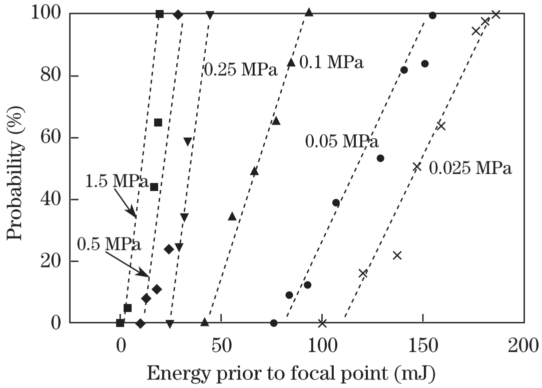

Fig. 1. Variation of probability of breakdown in air with laser energy prior to focal point at different pressures. Temperature of 300 K and quiescent mixture.

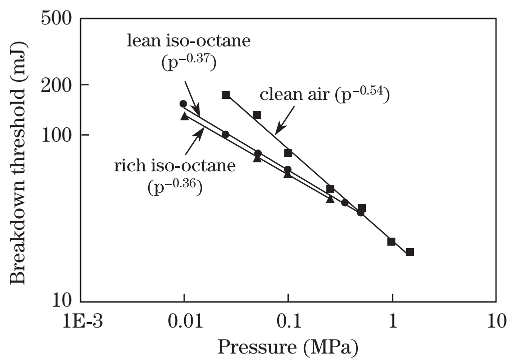

Fig. 2. Variation of breakdown threshold energy with pressure in clean air, lean, and rich isooctane-air mixtures. Quiescent mixture.

rich mixtures and the small difference is as likely to be due to shot-to-shot variations in laser energy as to equivalence ratio.

As with spark ignition, there is an initial rapid creation of a volume of high temperature plasma[3]. Behind this wave the hot plasma firsty contracts, as a consequence of the high rate of radiative energy loss. This decreases and eventually the kernel spreads radially by conduction. As the ionizing electron avalanche rapidly develops, the natural frequency of the plasma increases. If it becomes equal to that of the laser, the laser beam is unable to penetrate the plasma. This plasma frequency is given by[4]

$$\omega_{\rm p} = \left(\frac{n_{\rm e}e^2}{\pi m_{\rm e}}\right)^{1/2}. \quad (1)$$

It follows that, for energy transfer, the plasma frequency must be less than the laser frequency:

$$\omega_{\rm p} < c/\lambda, \quad (2)$$

where $n_{\rm e}$ is the number densities of the electron, c is the speed of light (2.998×10^{10} cm·s^{-1}), and λ is the laser wavelength (cm). In their experiment, the maximum plasma heating may occur at an electron number density of about $n_{\rm e} = n_{\rm c}/10$, where $n_{\rm c}$ is the critical electron number density, but several workers have taken this limiting value of $n_{\rm e} = n_{\rm c}/4$[5]. Another aspect of the generation of an energetic plasma is that the small volume of plasma absorbing the laser energy propagates up the laser beam as a wave, away from the original focus[6,7].

After breakdown, the spark expands asymmetrically which has been explained by three different view points including the breakdown wave theory, the radiation theory, and the detonation wave theory[1]. In the breakdown wave theory, it is assumed that a plasma kernel is created along the axis of the laser beam after breakdown. The kernel front facing the laser beam absorbs most of the laser energy that results in the strong ionization in the front of the kernel. The region of ionization expands away from the focus towards the lens. This mechanism determines the expansion of a spark kernel based on the rate at which the electron cascade is developed. From the radiative propagated wave theory, when a plasma kernel is formed by a laser beam it is heated to about 10^5–10^6K. It emits radiation and most of the radiation energy is in the far ultraviolet and has an absorption length of several millimeters. Thus, the hot plasma is transparent for thermal radiation and the radiation comes from the whole volume. To the surrounding cold gas layer, the absorption length is only a fraction of a millimeter, and although it is transparent to the laser beam, it absorbs the radiation from the hot plasma and is heated and ionized and becomes strongly absorbing to the laser light. The layer then is further heated to very high temperature and becomes a new layer of plasma in front of the initially formed plasma. As a result, the boundary of the plasma moves towards the laser. According to the detonation theory, cold layer is created by the shock wave after breakdown. When the spark forms it is heated rapidly to very high temperature, pressure, and expands. It generates a shock wave moving supersonically into the cold gas in all direction when this process is fast enough. The shock wave heats and ionizes the gas in its path. In the direction towards the lens, the newly ionized gas absorbs the laser beam and enhances the propagation of the shock.

However, the energy is no longer being supplied to the plasma when the laser pulse is ended. Under this circumstance the above mechanisms would be invalid. The plasma still expands until it gets equilibrium with the surrounding cold gas. In this case the approximate theory of spherical blast wave given by Taylor[8] can be used to predict the wave location, velocity, temperature, and pressure. The classical blast wave theory of Taylor[9] assumes an instantaneous transfer of energy into an infinitesimally small volume. A spherical shock wave is created and propagates outwards. The wave forces most of the gas within the shock front into a thin shell just inside that front. The shock pressure, velocity and temperature decrease with the front expands. The theory of Ref. [9] expresses the relationships between the shock wave radius $r_{\rm s}$ and the time t from the start of instantaneous energy deposition of the shock wave energy, E, as

$$r_{\rm s} = s(\gamma)t^{2/5}(E/\rho_0)^{1/5}, \quad (3)$$

$$v_{\rm s} = \frac{{\rm d}r_{\rm s}}{{\rm d}t} = s(\gamma)\frac{2}{5}t^{-3/5}(E/\rho_0)^{1/5}, \quad (4)$$

where $s(\gamma)$ is a constant of order unity that is a function of γ, the ratio of specific heats, while ρ_0 is the density ahead of the shock wave.

The development of a propagating flame may take several hundred μs and during this time the hot kernel also spreads further under thermal conduction. In the case of an electric spark, Bradley *et al.*[10] found the details of spreading by both shock-wave convection and conduction which are shown by the computations. In practice, it is possible to optimize the power–time profile for ignition. Taylor[11] suggested that good spreading of the kernel, first by the shock-wave, and then by conduction, can be obtained with a total spark duration of about 200 μs, combined with a higher power input during the first few microseconds.

As the spark front expands toward the laser, two contrarotating toroidal rings are generated in the vicinity of the laser beam axis leading to the development of the third lobe in a later time[1]. Bradley *et al.*[2] found that the shock-wave originates closer to the leading than to the trailing edge of the plasma ellipsoid is explained by the greater rate of energy absorption from the beam at the leading edge and its spatial exponential decay within the ellipsoid. Similarly, the center of the spherical rarefaction wave is always upstream of that of the hot kernel. The rarefaction wave produces a pressure gradient directed towards the center[10]. As in a Taylor instability[11], gas of lower density is accelerated more by this pressure gradient than is gas of higher density. As the rarefaction wave propagates outward the hot gas at the right is more persistently accelerated inwards, to generate two contra-rotating toroidal rings there. The aerodynamics of these changes is complex. Many authors have studied how the toroidal motion is generated by the computer and reviews of past work are available. Kono *et al.*[12] deemed that the inward flow was due to the "over expansion" of the shock-wave. The full line contours are computed isotherms that define the location of the hot gas forced into this location by the rarefaction wave. Most of the toroidal motion and the stagnation lines lie outside the region of the hot gas. Kravchik *et al.*[13,14] also provided similar computational demonstrations of how rarefaction waves generate toroids. Thiele *et al.*[15] provided that the geometry of the electrodes played an important part in determining that of the toroidal rings. In the near future, the numerical simulations have shown how the asymmetric deposition of laser energy and the pressure field generate a vortex and form the front lobe by Morsy *et al.*[16].

Figure 3(a) shows the elative position of shock and rarefaction waves and initiating plasma kernel and Fig. 3(b) shows kernel just after action of rarefaction wave. According to Fig. 3, the two toroidal rings are not symmetrical. The left is composed of lower density, high-velocity gas that dissipates its energy more rapidly and that the ellipsoidal geometry the duration of vorticity generation is shorter for the toroid at the left. It will decay more rapidly than that at the right. Later, the center line velocity toward the laser, generated by this toroidal ring, gives rise to a third lobe. However, the generation of the third lobe has not been fully explained. Spiglanin *et al.*[17] suggested that it might be due to the initial flow field created by the propagation of a radiation transport wave up the laser beam, arising from the high rate of energy transfer at the leading edge of the plasma and attributes the third lobe to gas velocities induced in the "over-expanded" region.

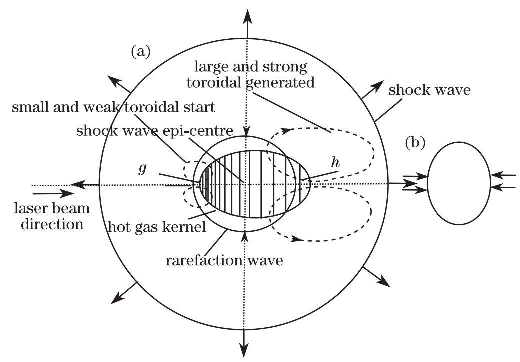

Fig. 3. (a) Relative position of shock and rarefaction waves and initiating plasma kernel, time is 15 μs; Closeness of shading on (a) is indicative of possible temperature distribution; (b) Kernels just after action of rarefaction wave.

Bradley *et al.*[2] found that in the early stages of kernel development the chain reactions necessary to sustain the expansion have not developed and the stretch rate of the reaction front is very high, since the kernel radius is very small. During this critical induction period, the propagation speed of the kernel decreases with the Karlovitz stretch factor. They also provide that at the lowest energy of 5.287 mJ there is insufficient chain branching during the induction period for a flame to develop and the kernel is quenched and then the energy increases to 5.419 mJ, which is sufficient for the induction reactions to initiate a propagating flame. Any further increase in energy increases the reaction rate toward the end of the induction period.

According to the blast wave model, it heats the surrounding gas when the blast wave expands. The requirement of ignition is that the wave can heat and maintain the gas temperature that exceeds the threshold ignition temperature, $T_{\rm ig}$, for a period longer than the induction time. Compared with the traditional electric spark ignition, this ignition mechanism is somewhat different[1]. The magnitude of the spark energy is small and the blast wave decays rapidly and the heated gas temperature cannot be sustained at its critical temperature longer than its chemical induction time. The ignition is purely and a thermal process and the subsequent combustion mechanisms are diffusion controlled, depending on the transport properties of the mixture as in normal flame propagation. The disturbance of the flow field by the decaying blast is so negligibly small that the flame kernel expands in an almost quiescent gas. In contrast with spark ignition, the laser-induced blast wave ignition is more dynamic. The blast expands after ignition with a coupled shock-chemical reaction front. In this case, the propagation of the blast front controls the combustion and simultaneously the blast front depends on the energy released by the chemical reactions. The flame detaches the blast front and continues to propagate outward as the blast decays. Shock-induced turbulence, after-shock recompression, the generation of the third lob during the spark expansion phase involves the rapid generation of an increased surface area at the plasma boundary and the associated high rate of stretch that can extinguish or prevent its the development of a propagating flame.

Akindele *et al.*[18] maintained that the initial stages of the development of the hot gas kernel in turbulent mixtures are similar to those in laminar mixtures for at least 100 μs after the onset of the spark. Abdel-Gayed *et al.*[19] described turbulent flame initiation. Initially, the smallest turbulent eddies are larger than the small plasma kernel. The kernel is not exposed to the full spectrum of turbulence and the main effect of turbulence is to convect the flame kernel bodily, without wrinkling its surface. The higher frequencies of turbulence increasingly wrinkle its surface and hence its rate of propagation into the unburned gas as the kernel grows.

Initially, the laminar Karlovitz number, $K_{\rm l}$, is dominant; later the turbulent Karlovitz number, K, is dominant. The latter is based on the mean strain rate, u'/λ, where u' is the rms turbulent velocity, $\delta_{\rm l}$ is Laminar flame thickness, $u_{\rm l}$ is unstretched laminar burning velocity and λ is the Taylor microscale:

$$K = \frac{u'}{\lambda}\frac{\delta_{\rm l}}{u_{\rm l}}. \quad (5)$$

One relationship of λ to the integral length scale, L, for isotropic turbulence gives[20]

$$K = 0.157(u'/u_{\rm l})^2 R_L^{-0.5}, \quad (6)$$

where R_L is the turbulent Reynolds number based on L. Sufficiently high values of K_L and of K can quench a flame[21].

In conclusion, although there are lots of similarities between laser-induced ignition and conventional ignition systems, laser-induced ignition has many potential benefits over the latter including the control over ignition location, ignition timing, ignition energy and its deposition rate can be easily carried out. Laser ignition offers the opportunity for sudden release of specific radicals and the onset of specific reactions which, in turn, may provide better means for controlling pollutant formation, ignition and flame stabilization especially for supper-lean combustion applications. And above all, laser ignition is capable of providing center ignition and/or multiple ignition sites that can be programmed to ignite a combustible mixture either sequentially or simultaneously thereby facilitating leaner operations[1]. Of course, various phenomena of laser-induced ignition have not been fully explained such as the generation of the third lobe and plenty of technical difficulties have not been overcame. But the potential and advantages make the laser-induced ignition more attractive in many practical applications and further studies leading to the development of laser-induced ignition systems are necessary.

This work was supported by the National Natural Science Foundation of China under Grant Nos. 50976100 and 51076138.

References

1. T. X. Phuoc, Optics and Lasers in Engineering **44,** 351 (2006).
2. D. Bradley, C. G. W. Sheppard, I. M. Suardjaja, and R. Woolley, Combustion and Flame **138,** 55 (2004).
3. H. L. Olsen, R. B. Edmonson, and E. L. Gayhart, J. Appl. Phys. **23,** 1157 (1952).
4. J. Sneddon, P. G. Mitchell, and N. S. Nogar, *Laser Induced Plasmas and Applications* L. J. Radziemski, D. A. Cremers (Eds.) (Dekker, New York, 1989) p. 367.
5. A. A. Hauer and A. Baldis, *Laser Induced Plasmas and Applications* L. J. Radziemski, D. A. Cremers (Eds.) (Dekker, New York, 1989) p.p. 105–161.
6. S. A. Ramsden and W. E. R. Davies, Phys. Rev. Lett. **13,** 227 (1964).
7. F. J. Weinberg and J. R. Wilson, Proc. R. Soc. London Ser. A **321,** 41 (1971).
8. G. I. Taylor. Proc. Roy. Soc. London, A **321,** 159 (1950).
9. G. I. Taylor, Proc. R. Soc. London Ser. A **201,** 159 (1950).
10. D. Bradley and F. K. K. Lung, Combust. Flame **69,** 71 (1987).
11. G. I. Taylor, Proc. R. Soc. London Ser. A **201,** 192 (1950).
12. M. Kono, K. Niu, T. Tsukamoto, and Y. Ujiie, Proc. Combust. Inst. **22,** 1643 (1989).
13. T. Kravchik and E. Sher, Combust. Flame **99,** 635 (1994).
14. M. Akram, AIAA J. **34,** 1835 (1996).
15. M. Thiele, S. Stelle, U. Riedel, J. Warnatz, and U. Maas, Proc. Combust. Inst. **28,** 1177 (2000).
16. M. H. Morsy and S. H. Chung, Proc. Combust. Inst. **29,** 1613 (2002).
17. T. A. Spiglanin, A. McIlroy, E. W. Fournier, R. B. Cohen, and J. A. Syage, Combust. Flame **102,** 310 (1995).
18. O. O. Akindele, D. Bradley, P. W. Mak, and M. McMahon, Combust. Flame **47,** 129 (1982).
19. R. G. Abdel-Gayed, D. Bradley, and M. Lawes, Proc. R. Soc. London Ser. A **414,** 389 (1987).
20. R. G. Abdel-Gayed, K. J. Al-Khishali, and D. Bradley, Proc. R. Soc. London Ser. A **391,** 393 (1984).
21. R. G. Abdel-Gayed and D. Bradley, Combust. Flame **62,** 61 (1985).